Zn K-edge EXAFS study of SILAR-grown zinc sulfide thin films

Seppo Lindroos,*[a]† Yves Charreire,[b] Tapio Kannianinen,[a] Markku Leskelä[a] and Simone Benazeth[c]

[a]*Department of Chemistry, University of Helsinki, PO Box 55, FIN-00014 University of Helsinki, Finland*

[b]*Université Paris VI, 5 Place Jussieu, F-75252 Paris cedex 05, France*

[c]*L.U.R.E. Laboratoire de Chimie Physique, Faculté de Pharmacie, Université de Paris Sud, F-91405 Orsay, France*

Zinc sulfide thin films grown by the successive ionic layer adsorption and reaction (SILAR) method have been characterized by extended X-ray absorption fine structure (EXAFS) measurements. The ZnS films were well crystallized even as-grown but annealing improved the crystallinity clearly. The films contained small amounts of oxygen and, according to the EXAFS results, oxygen in the SILAR-grown zinc sulfide thin films occurred as hydroxide ions both in the as-grown and in the annealed samples. The simulated radial distribution curves for two models, $Zn(OH)_2$/ZnS and ZnO/ZnS, were calculated to analyse the film composition. The ZnS thin films were also characterized by IR and electron spectroscopy for chemical analysis (ESCA) measurements.

The successive ionic layer deposition and reaction (SILAR) method based on a heterogeneous reaction on the solid/liquid interface was introduced by Nicolau in 1985.[1] The film growth in the SILAR method consists of four steps: in the first step cations are adsorbed on the substrate surface, in the second step all cations not adsorbed are rinsed away with purified water. The solvated anions enter the diffusion layer in the next reaction step and they react with the adsorbed cations. The ions which have not reacted are again washed away with a rinsing pulse in the fourth step. After a complete cycle a solid compound is formed on the surface of the substrate. By repeating these steps a thin film can be grown layer by layer. Hence the thickness of the film can be controlled directly by the number of deposition cycles.

The main advantage of the SILAR method is the possibility to deposit thin films that are impossible or difficult to grow using gas-phase methods. On the other hand, due to the layerwise growth of the thin film, the quality of the SILAR-grown films is comparable with films grown with other liquid-phase thin film deposition methods such as chemical bath deposition.[1–7] The SILAR technique has so far been used to grow II–VI compounds, such as ZnS.[1,2] The low temperature of the SILAR deposition allows also the use of temperature-sensitive precursors and substrates.[8]

One of the main problems in the SILAR process has been that some oxygen remains in the films owing to the aqueous growth conditions as confirmed by Rutherford backscattering spectroscopy (RBS) measurements.[2] According to the RBS results oxygen in the ZnS thin films is partly in water and partly bound to zinc as hydroxide or oxide. The form of oxygen, *viz*. oxide or hydroxide ion, in ZnS films is an interesting and important question when considering possible applications, and cannot be answered by Rutherford backscattering measurements only.

This study was carried out on one hand to analyse the oxygen concentration and coordination in the SILAR-grown films, *i.e*. whether the oxygen is bound to zinc as oxide or hydroxide. On the other hand, the purpose of this study was to compare the crystallinity of the SILAR-grown ZnS thin films to films grown by sputtering or gas-phase atomic layer epitaxy (ALE) methods.

The SILAR-grown ZnS thin films were also characterized by IR spectroscopy and ESCA measurements.

† Email: SLindroos@phcu.Helsinki.Fi

Experimental

Sample preparation

The zinc sulfide thin films were grown by the SILAR method with deposition equipment described earlier.[2] The aqueous precursor solutions used in the deposition were 0.1 M $ZnCl_2$ (pH = 5.3) and 0.05 M Na_2S (pH = 11.8). The immersion time was 20 s and the rinsing time was 100 s. The flow rate of the purified rinsing water was 600 ml min^{-1}. The ZnS thin films were grown on indium tin oxide (ITO)-covered glass substrates. During the growth the substrate was kept in an N_2 environment. Sample A was as-grown and sample B was annealed for 3 h at 500 °C in a nitrogen atmosphere. Both samples were deposited simultaneously and had thicknesses of 164 and 150 nm respectively. Chemical and physical characterization (chemical analysis, UV, XRD, RBS, SEM) of the SILAR-grown zinc sulfide thin films have been published earlier.[2]

For comparison to the SILAR-grown ZnS thin films, ZnO and ZnS powders, amorphous ZnS thin films prepared by sputtering and well crystallized thin film ZnS samples made by the ALE (atomic layer epitaxy) method in the Laboratory of Inorganic and Analytical Chemistry at the Helsinki University of Technology were also studied. The hexagonal forms of ZnS and ZnO were used.

EXAFS measurements

EXAFS experiments were performed at Lure (Orsay, France) using X-ray synchrotron radiation emitted by the DCI storage ring (1.85 GeV, 350 mA), in the EXAFS II installation. Data were collected using an Si(111) double crystal monochromator. Rejection of harmonics was not adopted. The EXAFS spectra of the thin films were recorded in a total electron yield mode[9] and measurements were made around the zinc K edge (9659 eV).

The EXAFS data analysis was carried out using a PC program written by Bonnin *et al*.[10] The background absorption features which are superimposed on the EXAFS oscillations were removed by linear extrapolation of the pre-edge. The normalized EXAFS signal $\chi(E) = [\mu(E) - \mu(E_0)]/\mu(E_0)$ was converted to wavevector k space, using $k = 2m(E - E_0)^{1/2}/\hbar$, where E_0 is the threshold energy close to the absorption edge of Zn (maximum of the first derivation of the spectrum).[11] For the $\chi(k)$ simulation, ΔE_0 is a parameter corresponding to a shift of the experimental value of E_0. Fourier transformation was performed using a Kaiser window in the range $2 < k < 13$ Å,

with a k^3 weighting.[12] After this the EXAFS contribution of the chosen coordination sphere was isolated by Fourier filtering and the experimental $\chi(k)$ was obtained by back-Fourier transform. After the back-Fourier transform to the k space the filtered EXAFS signal was k^3 weighted and Fourier transformed through a Kaiser window ($\tau=3$) on the spectral range extending from $k=4$ to *ca.* 12 Å^{-1}. Fitting was performed using the theoretical amplitude and phase functions of McKale *et al.*,[13] or experimental functions obtained by pure ZnS and ZnO reference compounds. The inelastic losses are usually approximated by the factor $\exp(-2r_j/\lambda)$ where λ is the inelastic mean free path. To take into account the k-dependence of this damping term we used the factor $\exp(-r_jL/k)$ where $L=2k/\lambda$. The relative mean squared static and thermal disorder between the central atom and the atoms in the jth coordination sphere is given by ${\sigma_j}^2$. To take into account this effect we introduced the factor $\exp(-{\sigma_j}^2k^2)$. The Fourier transform was made with respect to $\exp[2ikr_j+\phi_j(k)]$ where a phase shift $\phi_j(k)$ is needed to take into account the potentials due to both the central atom and the backscatterers. The phase shift is not totally simulated in the program and this causes a shift of all the peaks in $P(r)$ to closer to the origin by $\alpha_j=r_j-r'_j$, where r'_j is the observed distance in $P(r)$. From reference compounds ZnO and ZnS the shift was estimated to be 0.34 Å for oxygen and sulfur peaks. The parameters (L, σ) and (r, ΔE_0) are not independent. From earlier studies[12,14] on ZnS we had a good estimation for the values of the parameters at the beginning of the fit.

Table 1 Coordination shells (r/Å) around Zn in ZnS, ZnO and ε-$Zn(OH)_2$

shell	ZnS	ZnO	$Zn(OH)_2$
1	2.34 (4 S)	1.99 (4 O)	1.95 (4 O)
2	3.82 (12 Zn)	3.23 (12 Zn)	3.43 (4 Zn)
	3.91 (1 S)	3.25 (1 O)	
3	4.48 (9 S)	3.80 (9 O)	3.6–4.0 (4 O)
4	5.41 (6 S)	4.57 (6 Zn)	4.05–4.7 (8 O)
5	5.47 (6 S)	4.60 (6 O)	4.8–4.9 (4 Zn)

IR and ESCA measurements

The IR spectra were recorded using a Bruker IFS 85 spectrometer and for powder samples the CsBr pellet technique was used.

ESCA measurements were carried out with a Phi small spot ESCA 5400 electron spectrometer using unmonochromated Mg-Kα radiation.

Results and Discussion

The structural information used in this study is presented in Table 1 and the parameters used in EXAFS simulation and fits are presented in Table 2. Fig. 1 shows the $\chi(k)$ oscillation of the sample A and for comparison the $\chi(k)$ oscillation of a ZnS thin film sample deposited by the ALE technique. Fig. 2 shows the $k^3\chi(k)$ Fourier transform [radial distribution function $P(r)$] in k space in the range 2–13 Å^{-1} for the SILAR samples. The same curves for ZnS thin films prepared by the ALE method and by sputtering are presented for comparison. The peak located at 2.00 Å (shift of −0.34 Å from the correct distance) is at the exact position of sulfur atoms in the ZnS lattice. The first peak at 1.5 Å is due to oxygen and confirms thus the presence of oxygen in SILAR-grown films. The intensity of the second (Zn—S) peak of samples A and B in Fig. 2 is higher compared with that found in samples deposited by sputtering indicating a better crystallinity in SILAR samples. On the other hand, ZnS thin films deposited by ALE from the gas phase at elevated temperature and reduced pressure, are even better crystallized than SILAR samples. Annealing clearly approves the crystallinity of the SILAR-grown ZnS films.

Fig. 3 depicts the experimental radial distribution functions of ZnO and ZnS reference compounds (powder samples were studied by the transmission method) and simulated radial distribution function of the first six coordination spheres of ε-$Zn(OH)_2$. The simulation for $Zn(OH)_2$ was used because both commercial and several synthesized zinc hydroxide samples were found to be mixtures of $Zn(OH)_2$ and ZnO. The surroundings of zinc atoms in the ZnO and $Zn(OH)_2$ structures for the first neighbours (four oxygen atoms approximately at the same distance of 1.9 Å) are similar and were observed from this

Table 2 Bond lengths (r), coordination numbers (N), Debye–Waller factors (σ), L factors, edge shifts (ΔE_0) and standard deviations obtained by fitting EXAFS spectra for ZnS thin films (underlined values are fixed)

compound	shell	N	r/Å	σ/Å	L/Å^{-2}	ΔE_0/eV	$\sum(\Delta\chi^2/\chi^2)$	fitting used
ZnS sample A	1–O	0.75	1.91	0.071	1.50	—	28	experimental (19±2
	2–S	3.25	2.23	0.081	1.75	—		atom% oxygen)
ZnS sample B	1–O	1.15	1.99	0.064	1.50	—	29	experimental (29±3
(annealed)	2–S	2.85	2.30	0.068	1.75	—		atom% oxygen)
ZnS reference (ALE-	1–S	4	2.33	0.072	1.75	−4.7	26	McKale *et al.*[13] used
grown thin film)	2–Zn	12	3.83	0.115	1.75	−5.1		for Zn–S
	3–S	9	4.46	0.114	1.75	−1.1		
ZnO reference	1–O	4	1.90	0.069	1.50	−0.3	24	McKale *et al.*[13] used
(powder)	2–Zn	12	3.23	0.093	1.50	0		for Zn–O and
	3–O	9	3.80	0.093	1.50	0		Zn–Zn
$Zn(OH)_2$ reference	1–O	4	1.95	0.069	1.50	—	—	experimental
	2–Zn	4	3.43	0.093	1.50	—		
	3–O	4	3.80	0.093	1.50	—		
	4–O	4	4.20	0.093	1.50	—		
	5–Zn	4	4.90	0.093	1.50	—		
	6–O	4	4.60	0.093	1.50	—		
ZnO/ZnS	3–Zn	3.45	3.23	0.14	1.50	−7	—	McKale *et al.*[13]
	4–Zn	8.55	3.82	0.14	1.75	−7		
	5–O	2.59	3.80	0.14	1.50	−7		
	6–S	6.40	4.48	0.14	1.75	−7		
$Zn(OH)_2$/ZnS	1–O	1.15	1.92	0.064	1.50	−7	29	McKale *et al.*[13]
	2–S	2.85	2.31	0.068	1.75	−7		
	3–Zn	1.25	3.43	0.14	1.50	−7		
	4–Zn	8.55	3.83	0.14	1.75	−7		
	5–O	2.30	4.00	0.14	1.50	−7		
	6–S	6.40	4.48	0.14	1.75	−7		

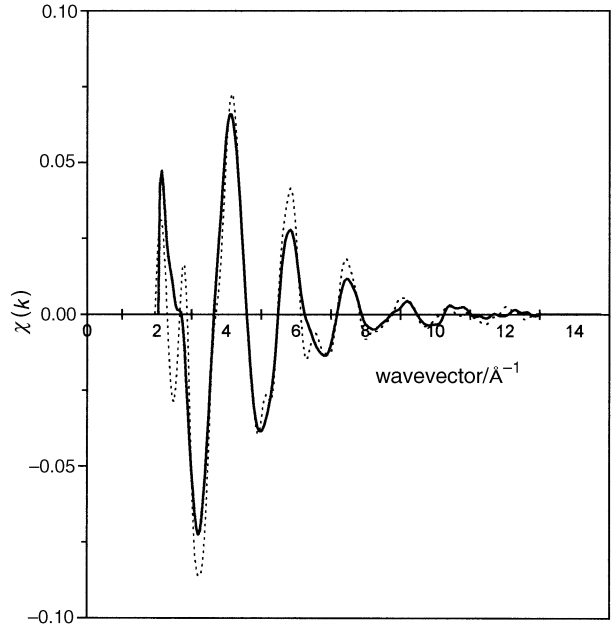

Fig. 1 A comparison of EXAFS oscillations $\chi(k)$ for SILAR-grown ZnS thin film sample A (···) and ALE-grown ZnS thin film reference (—) (prepared by the ALE group, Helsinki University of Technology)

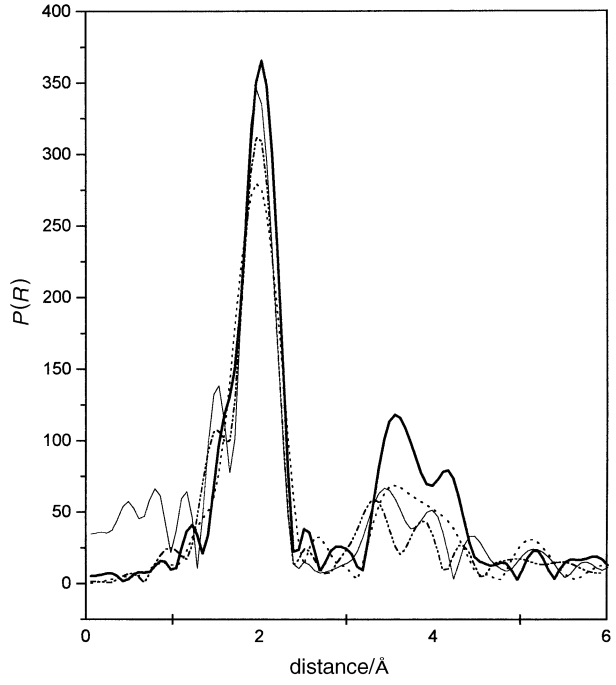

Fig. 2 Radial distribution curves $P(R)$ for SILAR thin films samples A (−··−) and B (—), ZnS film made by sputtering (− − −) and ZnS reference thin film prepared by ALE (▬)

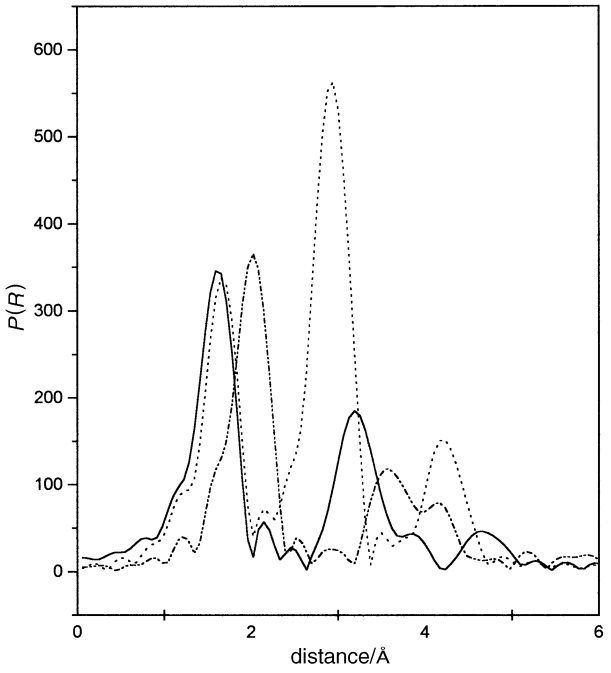

Fig. 3 Radial distribution function of ZnS (−··−) and ZnO (···) powders (transmission mode) and simulated $P(R)$ curve for $Zn(OH)_2$ (—)

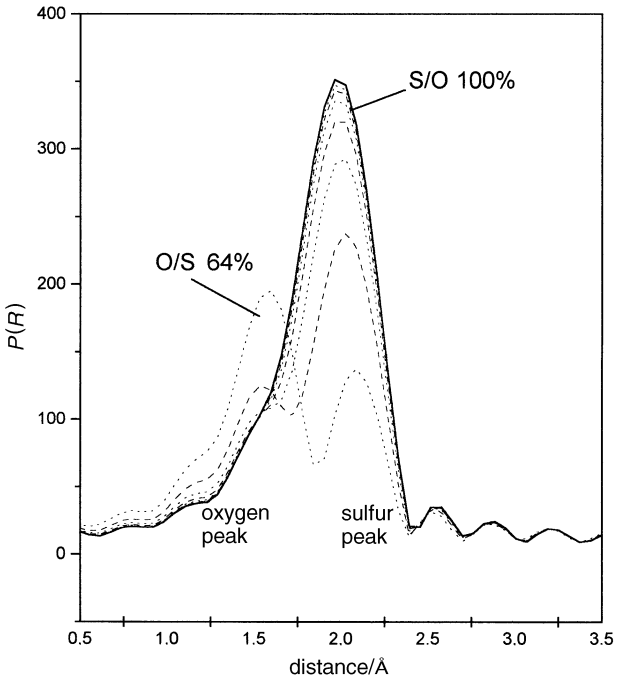

Fig. 4 The $P(R)$ curves for the ZnO/ZnS mixtures, where the percentage of ZnO increases from 0 to 1, 2, 4, 8, 16, and 64 atom%

Fourier transform (1.6 Å, shift −0.34 Å in Fig. 3). The Zn−OH bonding in the SILAR samples can be identified by the second coordination sphere. The peak of the four Zn atoms at 3.43 Å in $Zn(OH)_2$ structure can be easily separated from the peak of twelve Zn atoms at 3.23 Å in ZnO and 3.82 Å in ZnS structures.

To gain an idea about the sensitivity of EXAFS determination for the oxygen concentration the $P(R)$ curves for the ZnO/ZnS mixtures, where the percentage of ZnO increases from 0 to 1, 2, 4, 8, 16, and 64 atom% were studied (Fig. 4). Unfortunately there is a shoulder in the $P(R)$ curve of ZnS close to the oxygen peak at 1.5 Å (shift −0.34 Å). Almost 8 atom% of oxygen is required to observe a notable change in this shoulder. The oxygen peak is described only by 8 points (step in k space = 0.05 Å^{-1}, in R space = 0.061 Å) with the program used leading to poor spatial resolution and consequently low accuracy for determination of oxygen.

In this study the O/S ratio was first determined by the fit technique from the oxygen and sulfur peaks which correspond to a coordination number of four for the Zn atoms. In the second step the experimental $P(R)$ curves of the two thin films were compared with theoretical simulations made for two mixtures $(ZnO)_x/(ZnS)_y$ and $[Zn(OH)_2]_x/(ZnS)_y$ where x and y are determined from the O/S ratio. By simulation and fitting techniques the oxygen content can be estimated: the as-grown SILAR sample A contained 19 ± 2 atom% and the annealed sample B 29 ± 3 atom% oxygen. Annealing increases the EXAFS signal and increases the long-range order. The higher

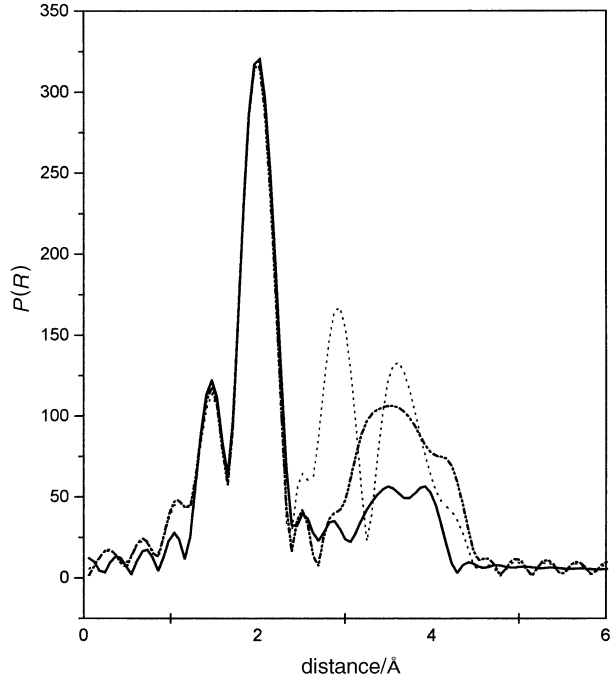

Fig. 5 The simulated radial distribution curve $P(R)$ for the first peaks (O, S, Zn, O and Zn) of the two models: mixed structures $Zn(OH)_2/ZnS$ (– – –) and ZnO/ZnS (···) with the experimental $P(R)$ for the sample B (—)

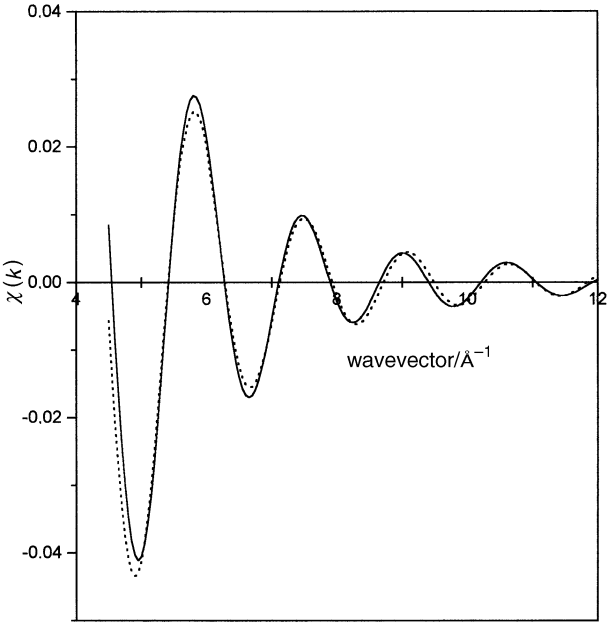

Fig. 6 Experimental (—) and simulated (···) EXAFS oscillations $\chi(k)$ of the first peak (oxygen) and the second peak (sulfur) of sample B

oxygen concentration after annealing is probably due to the increased surface roughness of the ZnS thin films. This enables the chemisorption or physisorption of atmospheric oxygen at the surface of zinc sulfide and hence an oxidized layer is formed on it. Also it has been observed, according to optical absorption studies, that the annealing of ZnS thin films can decrease the thickness of the film due to partial sublimation of ZnS even at low temperatures. The increase of oxygen content in the annealed SILAR-grown ZnS thin film can be attributed to the selective sublimation of ZnS.

The simulated radial distribution curves $P(R)$ for the first peaks (O, S, Zn, O and Zn) of the two models, mixed structures $Zn(OH)_2/ZnS$ and ZnO/ZnS, with the experimental $P(R)$ for the sample B are presented in Fig. 5. It can be concluded from the curves that the ZnO/ZnS model must be incorrect. The model $Zn(OH)_2/ZnS$ resembles more closely the experimental $P(R)$ but differences in intensity can be seen at larger distances.

Annealing increased both the EXAFS signal and the long-range order of the structure. Also, the resolution between oxygen and sulfur was better after annealing with the error for the determination of the O/S ratio being probably 30%. The errors indicated in Table 2 concerning the oxygen proportion correspond only to the interval explored during the fit. Nevertheless, we can conclude that both samples contain relatively significant amounts of oxygen. However the intensity of the EXAFS peak increases as the crystallinity of the sample increases. Owing to the lower crystallinity in sample A the EXAFS results are more uncertain than in sample B. On the other hand the better crystallinity in sample B may lead to a slight overestimate of the oxygen content.

Using the Fourier filtering technique, where one peak can be isolated in the experimental $P(R)$ curve, the corresponding coordination sphere can be analysed separately. The two first peaks (O, S) in the range 1.29–2.39 Å were isolated and the back Fourier transform of the selected $P(R)$ gave the $\chi(k)$ contribution of these two first peaks. The resulting 'filtered' EXAFS spectrum $[k^3\chi(k)]$ was then fitted. The result was a model where the coordination number is four and in the coordination sphere 19 and 29% of the atoms were oxygen in the A and B samples, respectively. Fig. 6 presents the experimental and simulated $\chi(k)$ curves for the isolated two first peaks of sample B and the fit was very good.

Fourier filtering between 2.39 and 4.23 Å gives the $\chi(k)$ oscillations of the next four peaks in the ZnO/ZnS mixture model and four or five peaks in the $Zn(OH)_2/ZnS$ mixture model (see Table 2). Fig. 7(*a*) and (*b*) show simulated $\chi(k)$ and $P(R)$ curves for these two models and for sample B. The simulation could not be made by the fit technique because there are too many free parameters but σ increased to 1.4 Å between the third and the sixth coordination spheres of the model. The simulations of the $P(R)$ and $\chi(k)$ curves are good enough to conclude that the SILAR films consist of a $ZnS/Zn(OH)_2$ mixture.

According to the XRD measurements, the ZnS and ZnS : Mn thin films prepared by SILAR were polycrystalline.[2,5] Annealing of the ZnS : Mn thin film at 500 °C in an N_2 atmosphere slightly increased the intensity of the [111] peak at $2\theta = 28.5°$ and decreased the FWHM.[5] The oxygen content of the SILAR-grown ZnS films, determined by RBS, varies from 10 to 20 atom%.[2] In the ZnS : Mn thin films the oxygen content decreased remarkably in the annealing process from 20 to 10 atom%.[5] The hydrogen content, determined by nuclear reaction analysis (NRA), of the ZnS : Mn thin films also decreased from about 10 atom% of the as-deposited film to 0.2–0.4 atom% of the annealed film.[5] The difference between the EXAFS and NRA results is possibly because the information depth of EXAFS is smaller compared with the information depth of NRA and RBS. On the surface of ZnS : Mn thin films there is a 10–20 nm thick layer where the hydrogen content is up to 2.5 atom% in the annealed films and even higher (*ca.* 5 atom%) in the as-grown films.[5] Oxygen in this surface layer exists most probably as water and zinc hydroxide. In the ZnS thin films grown by a chemical deposition method the films contained significant amounts of oxygen either as oxide ($ZnS_{0.5}O_{0.5}$) or as hydroxide [$ZnS_{0.5}(OH)$].[15]

According to the ESCA measurements of ZnS thin films grown by SILAR the Zn : S ratio was 1 : 1 and on an as-grown surface oxygen was detected. The oxygen content of the surface decreased remarkably after the sample was sputtered three times. It has been found that there is a thin oxidized layer on the surface of colloidal ZnS. The oxygen content of this surface layer diminished rapidly with depth and at a depth of 10 nm the oxygen signal halved in magnitude.[16]

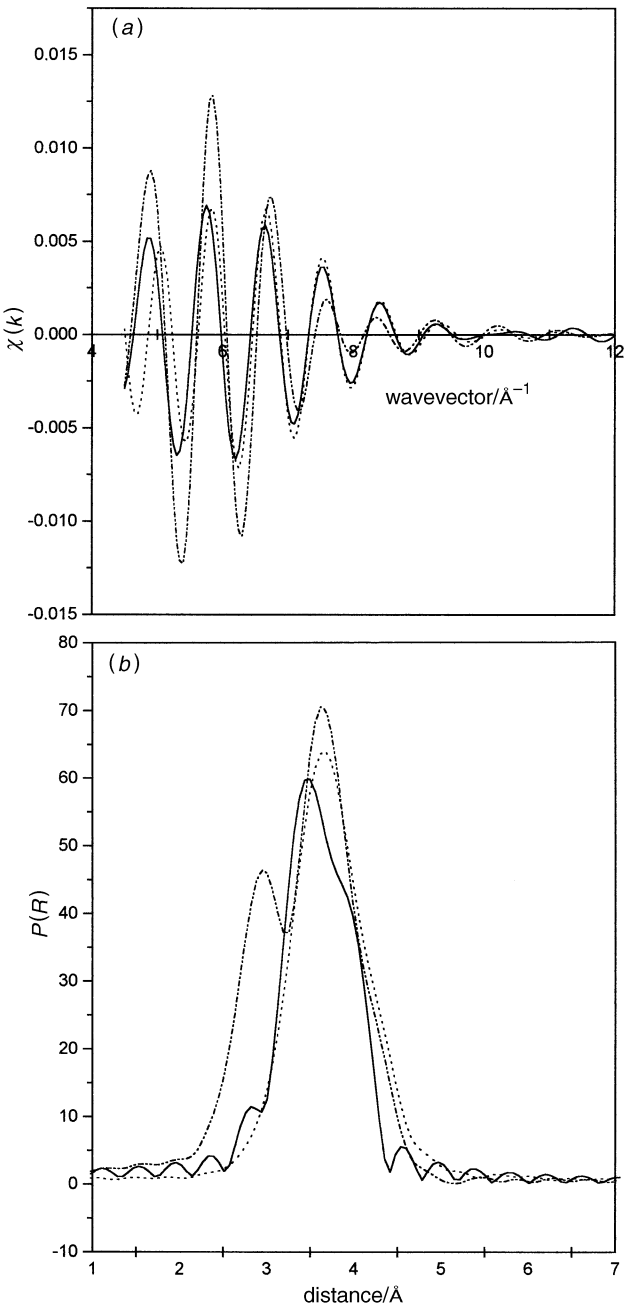

Fig. 7 (*a*) Comparison between the back Fourier transform of experimental radial distribution function and the $\chi(k)$ simulation of the third, fourth, fifth and sixth shells for the two mixture models $Zn(OH)_2$/ZnS and ZnO/ZnS: (—) back Fourier transform of filtered $P(R)$ of sample B; ($-\cdots-$) simulation of *a priori* ZnO/ZnS model; (···) simulation of *a priori* $Zn(OH)_2$/ZnS model. (*b*) Radial distribution function $P(R)$ of EXAFS oscillations $\chi(k)$ of Fig. 7(*a*) for k space: (—) the experimental curve; ($-\cdots-$) *a priori* ZnO/ZnS model; (···) *a priori* $Zn(OH)_2$/ZnS model.

In the IR spectra of the ZnS thin films deposited by SILAR the Zn—S (zinc sulfide) and Zn—O (zinc oxide) stretch vibration peaks were found at 302.8 and 468.6 cm^{-1}, respectively. The broad moisture peak at 3416 cm^{-1} possibly masks two narrow peaks at *ca.* 3670 and 3620 cm^{-1} and two broad peaks at *ca.* 3555 and 3440 cm^{-1} of hydroxy groups.[17,18] The water bending peak at 1646.1 cm^{-1} was also identified. The Zn—OH stretching peak at 648 cm^{-1} [19] could not be observed. The broad absorption band at 1457–1377 cm^{-1} assigned as Zn—O(HCO_2) by Gärd *et al.*[20] was observed in the spectra. As a conclusion of the IR measurements the SILAR-grown ZnS thin films contain oxygen as zinc oxide and carbonate and water was also found in the films. The IR spectrum can be used only qualitatively to analyse oxygen since addition of only 1% ZnO to ZnS powder has been known to give a strong absorption at 460 cm^{-1}.[21]

Conclusions

The oxygen content and the form of the oxygen ion in the SILAR-grown zinc sulfide thin films has been determined by EXAFS measurements and simulation of ZnO/ZnS and $Zn(OH)_2$/ZnS mixture models. The ZnS thin films prepared by SILAR contain 10–30% oxygen. Near the surface of the film, in the volume where EXAFS information is originated, the oxygen is bound more probably as Zn—OH than as Zn—O both in as-grown and annealed films. The absence of the peak corresponding to the twelve Zn—Zn distances at 3.23 Å, characteristic of ZnO, confirms this conclusion. The crystallinity of the SILAR-grown ZnS thin films is fully compatible with the ZnS thin films grown by the ALE method at higher temperatures.

We thank Prof. J. Väyrynen (University of Turku) and Mrs. H. Lepesant (Ecole National Superieure de Chimie de Paris) for ESCA and IR measurements, respectively. The research has been supported by Academy of Finland and Technology Advancement Centre of Finland (TEKES).

References

1 Y. F. Nicolau, *Appl. Surf. Sci.*, 1985, **22/23**, 1061.
2 S. Lindroos, T. Kanniainen and M. Leskelä, *Appl. Surf. Sci.*, 1994, **75**, 70.
3 Y. F. Nicolau and J. C. Menard, *J. Cryst. Growth*, 1988, **92**, 128.
4 Y. F. Nicolau and J. C. Menard, *J. Appl. Electrochem.*, 1990, **204**, 1063.
5 S. Lindroos, T. Kanniainen, M. Leskelä and E. Rauhala, *Thin Solid Films*, 1995, **263**, 79.
6 R. Ortega Borges, D. Lincot and J. Vedel, *11th E.C. Photovoltaic Solar Energy Conference, Montreux*, 1992, p. 862.
7 J. M. Doña and J. Herrero, *J. Electrochem. Soc.*, 1994, **141**, 205.
8 S. Lindroos, T. Kanniainen and M. Leskelä, *J. Mater. Chem.*, 1996, **6**, 1497.
9 G. Tourillon, E. Dartyge, A. Fontaine, M. Lemonnier and F. Bartol, *Phys. Lett. A*, 1987, **121**, 251.
10 D. Bonnin, P. Kaiser, C. Fretigny and J. Desbarres, *Structures Fines d'Adsorption des Rayons X en Chimie*, Ecole du C.N.R.S., Orsay, 1989, vol. 3, part 2.
11 H. D. Abruña, J. H. White, M. J. Albarelli, G. M. Bommarita, M. J. Bedzyk and M. McMillan, *J. Phys. Chem.*, 1988, **92**, 7045.
12 Y. Charreire, A. Marbeuf, G. Tourillon, M. Leskelä, L. Niinistö, E. Nykänen, P. Soininen and O. Tolonen, *J. Electrochem. Soc.*, 1992, **139**, 619.
13 A. G. McKale, B. W. Veal, A. P. Paulikas, S.-K. Chan and G. S. Knapp, *J. Am. Chem. Soc.*, 1988, **110**, 3763.
14 Y. Charreire, D.-R. Svoronos, I. Ascone, O. Tolonen, L. Niinistö and M. Leskelä, *J. Electrochem. Soc.*, 1993, **140**, 2015.
15 B. Mokili, M. Froment and D. Lincot, *J. Phys. IV*, 1995, **5**, C3.
16 D. T. Atkins and R. M. Pashley, *Langmuir*, 1993, **9**, 2232.
17 K. Atherton, G. Newbold and J. A. Hockey, *Discuss. Faraday Soc.*, 1971, **52**, 33.
18 W. Hertl, *Langmuir*, 1988, **4**, 594.
19 J. W. Kauffman, R. H. Hauge and J. L. Margrave, *J. Phys. Chem.*, 1985, **89**, 3541.
20 R. Gärd, Z-X. Sun and W. Forsling, *J. Colloid Interface Sci.*, 1995, **169**, 393.
21 Q. Yitai, S. Yi, C. Qianwang and C. Zuyao, *Mater. Res. Bull.*, 1995, **30**, 601.

Paper 6/08383; *Received* 13*th December*, 1996